Theoretical study of *cis*platin adsorption on silica

S. Simonetti [a,b,*], A. Díaz Compañy [a], G. Brizuela [a], A. Juan [a]

[a] *Departamento de Física and IFISUR, Universidad Nacional del Sur-CONICET, Av. Alem 1253, 8000 Bahía Blanca, Argentina*
[b] *Departamentos de Ciencias Básicas e Ingeniería Mecánica, Universidad Tecnológica Nacional, 11 de Abril 461, 8000 Bahía Blanca, Argentina*

ARTICLE INFO

ABSTRACT

The adsorption of *cis*platin and its complexes, *cis*-[PtCl(NH$_3$)$_2$]$^+$ and *cis*-[Pt(NH$_3$)$_2$]$^{2+}$, on a SiO$_2$(1 1 1) hydrated surface has been studied by the Atom Superposition and Electron Delocalization method. The adiabatic energy curves for the adsorption of the drug and its products on the delivery system were considered. The electronic structure and bonding analysis were also performed. The molecule–surface interactions are formed at expenses of the OH surface bonds. The more important interactions are the Cl–H bond for *cis*-[PtCl$_2$(NH$_3$)$_2$] and *cis*-[PtCl(NH$_3$)$_2$]$^+$ adsorptions, and the Pt–O interaction for *cis*-[Pt(NH$_3$)$_2$]$^{2+}$ adsorption. The Cl p orbitals and Pt s, p y d orbitals of the molecule and its complexes, and the s H orbital and, the s and p orbitals of the O atoms of the hydrated surface are the main contribution to the surface bonds.

© 2011 Elsevier B.V. All rights reserved.

1. Introduction

*Cis*platin (*cis*-diaminedichloroplatinum [II]) is a coordination compound, used in the treatment of several solid tumors [1,2]. It is well known square planar complex with chemical formula *cis*-[Pt(NH$_3$)$_2$Cl$_2$] first described by Michel Peyrone in 1844. The structure was elucidated by Alfred Werner nearly 50 years later in 1893.

*Cis*platin in water dissolution, hydrolyse easily [3], settling down a balance between the *cis*platin and its products *cis*-[Pt (NH$_3$)$_2$Cl(H$_2$O)]$^+$ (monoacuo cisplatin), cis-[Pt(NH$_3$)$_2$(H$_2$O)$_2$]$^{2+}$ (diacuo *cis*platin) and the hydroxo complexes *cis*-[Pt(NH$_3$)$_2$Cl(OH)], *cis*-[Pt(NH$_3$)$_2$(OH)$_2$] and *cis*-[Pt(NH$_3$)$_2$(OH)(H$_2$O)]$^+$. This balance depends on Cl$^-$ concentration and pH [4–8]. Aiming to predict potentially active species in the mode of action of the anticancer drug *cis*platin studies have focused on the hydrolysis of one or both platinum–chloro bonds of the drug [9–13].

*Cis*platin and its hydrolysis products exhibit a great pharmacological effect. Nevertheless, they have significant adverse side effects [14,15]. The optimization of the dosing and delivery schedule can potentially minimize adverse effects while maintaining efficacy [16,17]. Studies have shown that silica matrixes could improve delivery systems for implants [18,19].

Simulation techniques supply useful information for the study of the delivery systems. Studies about *cis*platin and *cis*platin analogs are frequently explored by computational methods [20–23].

In order to perform pharmacological studies and shed more light in the drug liberation and action mechanisms, it is necessary a previous study of the adsorption properties of the *cis*platin and its complexes in the selected carrier matrix.

The anti-tumor properties of square planar platinum (PtY$_2$L$_2$) complexes have been studied with various techniques. The properties of these complexes were investigated by focusing on the ligand exchange reactions via the interaction between the metal and ligands/solvents. The ligand exchange reactions of these Pt(II) complexes are suggested to proceed via a five-coordinated transition state with an axial metal–ligand interaction [24–29]. These ligand exchange processes are also characterized by electron density transfers from the neutrally and negatively charged ligands to the central Pt(II) metal and the leaving L groups. The charge values of the central metal are dependent on the contribution of the charges transferred from the electron pair of the ligands. Since the unoccupied dx^2–y^2 orbital interacts with the lone pair orbitals of the ligands, the structural characteristic of Pt(II) stereochemistry is the tendency to form square planar Pt(II) complexes. In terms of the reaction mechanisms associated with the ligand exchanges at the planar d^8 center, some studies [24–29] reported that the reaction proceeds via a five-coordinated transition state ([PdL5]) with a D3h (C2v)-trigonal bipyramidal structure. The stationary steps in the mechanism for the *cis*platin hydrolysis were characterized by Zhang et al. [25] and Costa et al. [27]. Although the reaction mechanisms for the ligand exchange of the Pt(II) complexes have been studied by some groups, the potential energy surfaces through the ligand exchange processes and the electronic structure and

* Corresponding author at: Departamentos de Ciencias Básicas e Ingeniería Mecánica, Universidad Tecnológica Nacional, 11 de Abril 461, 8000 Bahía Blanca, Argentina. Tel.: +54 0291 4595141/4555220; fax: +54 0291 4595142.
E-mail address: ssimonet@uns.edu.ar (S. Simonetti).

bonding considerations have not yet been investigated at a fundamental level.

In the present study, we analyze theoretically the adsorption of *cis*platin and its products, $[PtCl(NH_3)_2]^+$ and *cis*-$[Pt(NH_3)_2]^{2+}$, in a silica hydrated matrix. The minimum energy geometries of *cis*platin and its complexes are calculated by the Atom Superposition and Electron Delocalization (ASED) method. The changes in the electronic structure and the chemical bonding are also addressed.

2. Computational method

Our calculations were performed using the ASED method [30–33]. This method is a modification of the extended Hückel Molecular Orbital method (EHMO) implemented with the YAeHMOP program (Yet Another extended Hückel Molecular Orbital Package) [34].

The ASED method is a semi-empirical method, which makes a reasonable prediction of molecular and electronic structure. The EHMO method in its original form is not able to optimize geometries correctly as it lacks repulsive electrostatic interactions. This deficiency can be overcome by introducing a two-body electrostatic correction term [35].

The ASED theory is based on a physical model of molecular and solid electronic charge density distribution functions [33–36].

The adiabatic total energy values were computed as the difference between the electronic energy (E) of the system when the drug is at finite distance on the surface and the same energy when that drug is far away from the solid surface:

$$\Delta E_{\text{Abs, total}} = E(\text{carrier} + \text{drug}) - E(\text{carrier}) - E(\text{drug}) + E_{\text{repulsion}}$$

The repulsive energy was computed taking into account all atom–atom interactions.

To understand the drug–carrier interactions we used the concept of density of states (DOS) and crystal orbital overlap population (COOP) curves. The DOS curve is a plot of the number of orbitals per unit volume per unit energy. The COOP curve is a plot of the overlap population weighted DOS vs. energy. The integration of the COOP curve up to the Fermi level (E_f) gives the total overlap population of the bond specified and it is a measure of the bond strength.

3. The drug–carrier system

We have selected as a drug–carrier hydrated silica. SiO$_2$, is found in various crystalline and amorphous forms and a considerable amount of research has been devoted in the past to characterize the surface structure of amorphous silica, particularly by using the infrared spectroscopy to identify the different OH species present at the surface. Many of the properties of silica depend on the chemical composition and structure of its surface. It is now accepted that the surface Si atoms tend to have a complete tetrahedral configuration and, in an aqueous medium their free bonds become saturated with hydroxyl groups forming silanol groups (=Si–OH), denoted as single or isolated groups, or geminal silanol groups (>Si(OH)$_2$). We have simulate completely hydrated silica by considering it comparable to the (1 1 1) surface of β-cristobalite, in which each surface Si atom is connected to a single silanol group [37]. The crystal structure of β-cristobalite is based on networks of corner-connected SiO$_4$ tetrahedra, with non-collinear Si–O–Si bonds forming bond angles of approximately 147°. This type of modeling has been useful for adsorption studies of several molecules [38,39].

We used a supercell of 209 atoms: 54 Si distributed in six layers, 128 O atoms and 27 H atoms. Every Si atom completes its tetrahedron with O atoms. As a starting geometry for the surface, we used the following distances: Si–Si, 5.07 Å; Si–O (surface), 1.5 Å; O–O (bulk), 2.53 Å; O–H, 0.96 Å and H–H, 5.07 Å. In order to
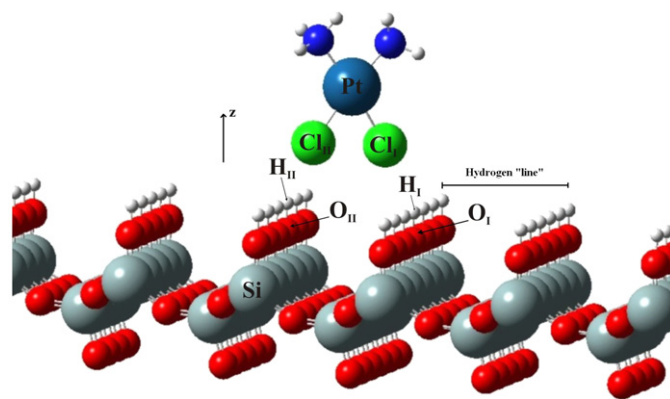

Fig. 1. Schematic view of the *cis*platin adsorption geometry.

reproduce the surface, this cell is extended in two dimensions parallel to the surface. All dangling bonds were saturated with additional H atoms.

The starting point for the calculation was the *cis*platin structure (see Fig. 1) taken from experimental data [40,41]. Initial optimization of *cis*platin agreed with the findings of several theoretical studies [42] giving a C$_{2v}$ minimum with a distorted square–planar coordination about. The in-plane N–H groups are aligned toward Cl, resulting in (N–H)–Cl distances and angles of 2.41 Å and 113°. The electrostatic potential shows a highly polar molecule more positive on the amino group and negative on the chlorine atoms. The Pt is close to neutral.

During the calculations, the structures of both molecule and substrate were optimized at steps of 0.02 Å and convergence in energy of 0.01 eV. We found optimized distances for the equilibrium geometry structures that are in a good accordance with previous experimental and computational studies [43]. Different both molecule/fragments orientations and adsorption sites on the hydrated silica surface was taken in order to obtain the optimum adsorption geometry and the preferential adsorption site. From the energy mapping we have detected three different possible adsorptions sites, named A, B and C, that contain two terminal Si–OH available to interact with Cl atoms from *cis*platin molecule/fragment. These sites are indicated in Fig. 2. For the three possible sites we have optimized the molecule/fragment
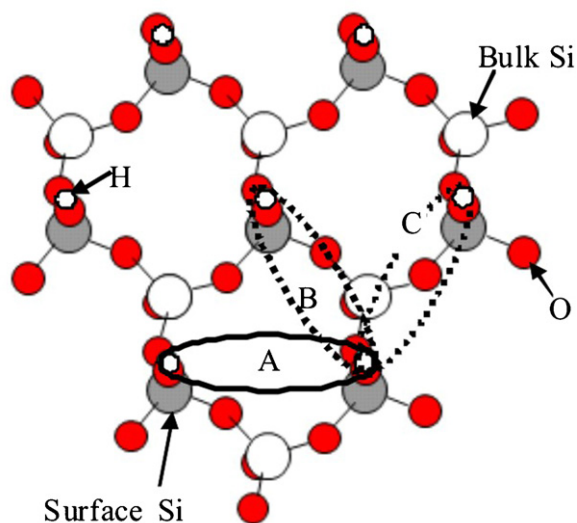

Fig. 2. Surface model of β-crystobalite showing the arrangement of surface hydroxyls, surface and bulk silicon atoms. The pairs of OH available to interact with Cl atoms from *cis*platin are indicated by A, B or C.
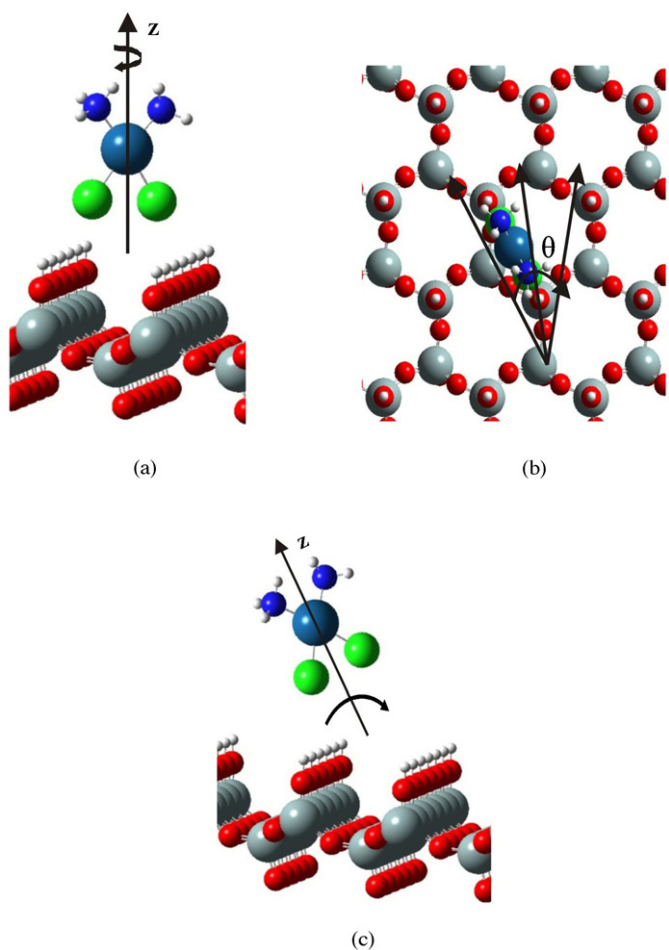
Fig. 3. Optimization parameters on the silica surface after adsorption on sites A, B or C.

Fig. 4. Adiabatic total energy curves for the (a) *cis*platin–silica system, (b) *cis*-[PtCl(NH$_3$)$_2$]$^+$–silica system and (c) *cis*-[Pt(NH$_3$)$_2$]$^{2+}$–silica system.

surface-distance, z (see Fig. 1), the rotation angle around an axis entering the surface and a rotation angle parallel to the H line (see Fig. 3). In each case we have also moved the *cis*platin species along the line of Si–OH on the surface.

As mentioned before, we have mapped the location of the molecule and their fragments on the silica surface, following different rotation angles and adsorbate translations at steps of 0.05 Å (see Figs. 2 and 3). After the minima height was obtained (z direction in Fig. 1), the molecule/fragments were rotated around an axis through Pt atom (see Fig. 3(a)) and, tilted and rotated at different angles (0°, 30°, 60° and 90°) (see Fig. 3(b)). Finally, we have improved the adsorption geometry considering the adsorption of the molecule, rotated at different angles in the surface plane (θ = 30°, 60°, 90°, 120° and 150°) (see Fig. 3(c)).

We have computed the adiabatic energy of the system absorbing the drug on the SiO$_2$(1 1 1) hydrated surface. We have obtained the energy curves, initially for the *cis*platin molecule and then, considering the removal of one and the two chloro atoms of the molecule, in order to analyze the hydrolysis products adsorption. In consequence, we have studied the major electronic interactions between the drug/fragments and the silica surface.

4. Results and discussion

We have found that the OH groups provide a favourable zone for the adsorption of the *cis*platin and their fragments obtained on it, the position of minimum energy. The most favourable corresponds to the ve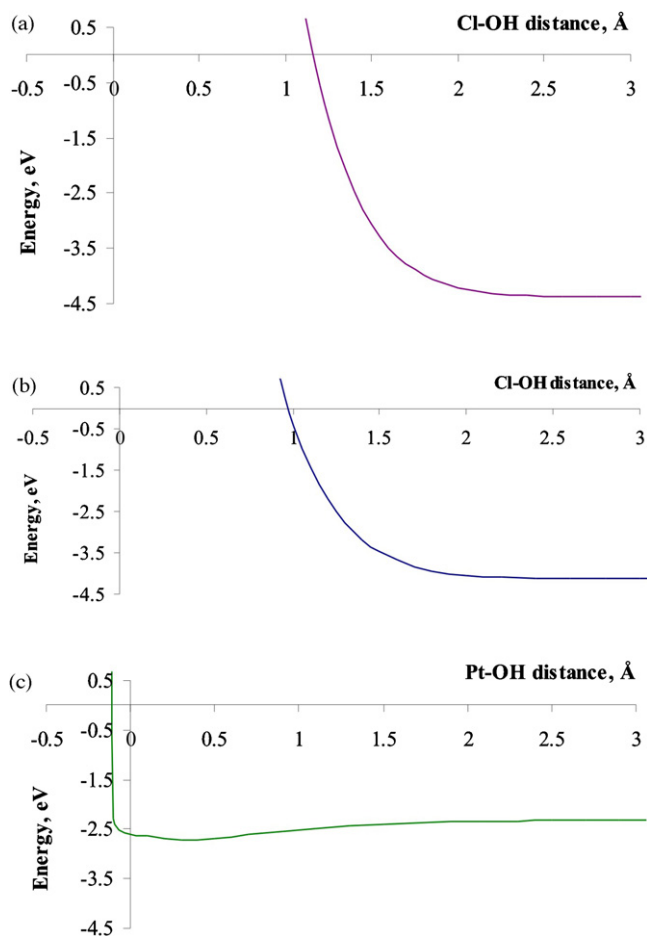rtical adsorption of the molecule and its fragments in a way that the Cl atoms are closer to the OH groups of the hydrated silica surface in the A configuration (see Fig. 2). These results are in agreement to the hydrolysis reactions data for *cis*platin found in the literature [3,23,44,45] and we have found the optimized adsorption parameters of the equilibrium geometrical structures that are in a good accordance with experimental and computational previous studies [43, and references therein]. Many quantum chemical studies have focused on the hydrolysis of one or both Pt–Cl bonds of *cis*platin and arrived at the conclusion that both the second and third hydrolysis are strongly endothermic and thus neither *cis*-[Pt(NH$_3$)$_2$(OH$_2$)$_2$]$^{2+}$ nor *cis*-[Pt(NH$_3$)$_2$(OH$_2$)(OH)]$^+$ are involved in the anticancer activity of *cis*platin [45].

The adsorption energies for *cis*platin and its complexes are shown in Fig. 4. For *cis*-[PtCl$_2$(NH$_3$)$_2$] adsorption, the system become stable considering the OH–Cl distances below of 1.2 Å (see Fig. 4(a)). For distances shorter than 1.2 Å, the molecule–surface repulsion is evident. When we computed the energy of the system considering the *cis*platin complexes adsorption, for the [PtCl(NH$_3$)$_2$]$^+$ complex, we can see in Fig. 4(b) that the system is stable when this complex is from 1.0 Å above the surface; while for the *cis*-[Pt(NH$_3$)$_2$]$^{2+}$ adsorption, the system is more stable near the surface (see Fig. 4(c)) but the energy has lower value compared to *cis*-[PtCl$_2$(NH$_3$)$_2$] and [PtCl(NH$_3$)$_2$]$^+$–silica systems. Analyzing the energy plots for the three systems, we can see that the *cis*-[PtCl$_2$(NH$_3$)$_2$]–silica system is the most stable between 3.2 and 1.8 Å, while [PtCl(NH$_3$)$_2$]$^+$–silica system is the most stable between 1.6 and 1.4 Å, and the *cis*-[Pt(NH$_3$)$_2$]$^{2+}$–silica system is the most stable from 1.3 Å toward the surface. Following this energy analysis, we could imagine a hypothetical way on the
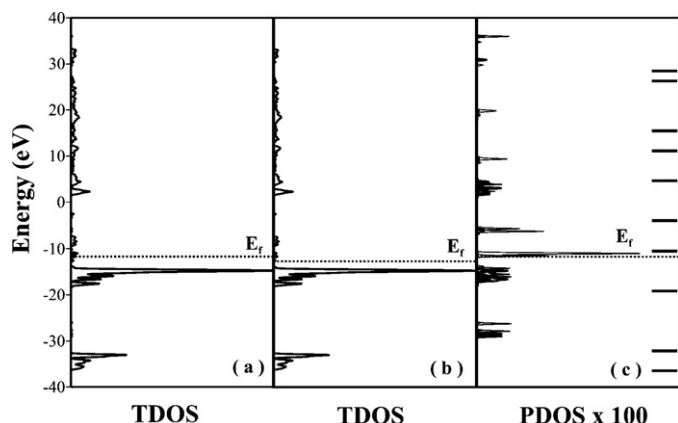
Fig. 5. (a) Total DOS for the *cis*platin–silica system, (b) total DOS for the isolated silica carrier and (c) projected DOS for the *cis*platin molecule adsorbed on the silica surface. The horizontal solid lines indicate the orbital energies the isolated *cis*platin molecule.

molecular approach to the surface losing the first chloro atom (the hydrolysis process). On the other hand, considering the favourable adsorption energy values for the *cis*-[PtCl$_2$(NH$_3$)$_2$] molecule and the [PtCl(NH$_3$)$_2$]$^+$ complex, these could be adsorbed before the partial or the total removal of the Cl atoms respectively, when the molecule or the complex are located at 3.2–2 Å to the surface, settling down the hoped balance between the *cis*platin and its products [6–8].

Fig. 5(a) shows the density of states (DOS) curve for the *cis*-[PtCl$_2$(NH$_3$)$_2$]–silica system. If we compare with Fig. 5(a) and (b) that corresponding to the silica isolated solid, the changes are small because the molecule presence is almost negligible. The contributions to the DOS of the *cis*platin orbitals are evident if those are magnified by a factor of hundred, in Fig. 5(c). The horizontal sticks display the energy of the molecular orbitals in the isolated *cis*platin molecule. We can see the dispersion corresponding to the bands, these are due to the interaction with the hydrated silica surface. After adsorption the bands are spread over and a portion of its DOS is pushed above the Fermi level. The value of the Fermi energy (E_f) of the *cis*-[PtCl$_2$(NH$_3$)$_2$]–silica system is −11.70 eV and it changes slightly with respect to the isolated silica (E_f = −12.70 eV). The states below the Fermi level mainly correspond to the silicon conduction band.

According to the most favourable adsorption energies ranges for the three studied systems, we have selected one configuration of each system in order to perform the electronic structure analysis and bonding considerations.
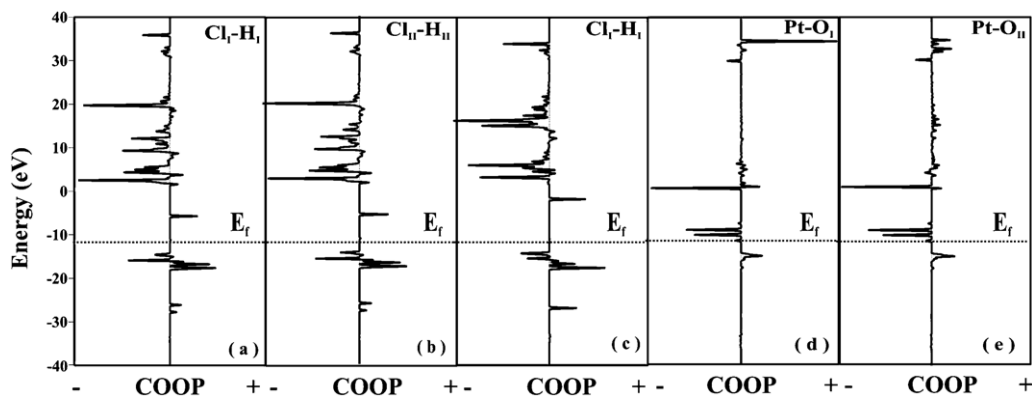
For *cis*-[PtCl$_2$(NH$_3$)$_2$]–silica system we have selected the geometry corresponding to the molecule–surface distance (OH–Cl distance) of 2.2 Å. For this configuration, each Cl atoms to the *cis*platin have interactions with the H atoms of two nearest neighbour OH groups of the hydrated surface. The existence of these bonds is confirmed by the bond population, the Cl–H overlap populations (OPs) are 0.020 and 0.004, respectively. The COOP curves can be seen in Fig. 6(a) and (b). These curves present bonding and antibonding peaks below the Fermi Energy level (E_f). The integration up to the Fermi level gives the total OP for the Cl–H bonding. The Cl–O interactions are almost negligible. There is no evidence of Cl–Si interactions.

For *cis*-[PtCl(NH$_3$)$_2$]$^+$–silica system we have selected the geometry corresponding to the complex located at 1.6 Å to the surface. For this configuration, the Cl atom has an interaction with an H atom of an OH group of the surface. The Cl–H bond population is 0.005. The interaction is small; the COOP curves can be seen in Fig. 6(c). No other important interactions were observed.

For *cis*-[Pt(NH$_3$)$_2$]$^{2+}$–silica system we have considered the geometry corresponding to the complex positioned at 0.3 Å to the surface. When the two chloro atoms are removed, the most favourable interactions occur between the Pt and the O atoms of the OH groups. The Pt–O OP values are between 0.004 and 0.04. Fig. 6(d) and (e) shows the major Pt–O COOPs curves. On the other hand, the Pt–H interactions have very small OP values.

The adsorption of the drug is possible because it is produced a rearrangement of the electronic densities of the solid surface and the *cis*platin atomic orbitals. The major changes are summarized in Table 1.

For *cis*-[PtCl$_2$(NH$_3$)$_2$]–silica system, the orbital populations of the O and H atoms of the surface decrease less than 1%, while de s and p orbitals of the Cl atoms decrease 0.5% and 20%, respectively. The s, p and d orbital population of the Pt atom decrease 32%, 5% and 85%, respectively. Then, for *cis*-[PtCl$_2$(NH$_3$)$_2$]–silica interaction, the most affected are the p Cl orbital and the s and d orbital populations of the Pt atom.

For *cis*-[PtCl(NH$_3$)$_2$]$^+$–silica system, the 1 s H population of OH superficial group decrease a 1% while the corresponding s and p orbital populations of the O atom increase 0.5% and 1.3%, respectively. The s and p orbitals of the Cl atom decrease 0.8% and 7%, respectively while the s, p and d orbitals of the Pt atom decrease 32%, 26% and 88%, respectively. Therefore, the atomic orbitals of the *cis*-[PtCl(NH$_3$)$_2$]$^+$ complex are the most affected after adsorption.

For *cis*-[Pt(NH$_3$)$_2$]$^{2+}$–silica system, the 1 s H population of OH surface group decrease a 0.9% while the corresponding s and p orbital populations of the O atom increase 0.1% and 0.7%, respectively. The s, p and d orbitals of the Pt atom decrease

Fig. 6. COOP curves for (a) and (b) the Cl–H interactions in the *cis*platin–silica system, (c) the Cl–H interaction in the *cis*-[PtCl(NH$_3$)$_2$]$^+$–silica system, (d) and (e) the Pt–O interactions in the *cis*-[Pt(NH$_3$)$_2$]$^{2+}$–silica system.

Table 1
Orbital occupations, net charges and overlap population (OP) for the atoms whose participate in the interactions.

	Orbital occupation			Charge	Bond	OP
	s	p	d			
H_I	0.6009			0.3991[a]	O_I–H_I	0.610[a]
	0.5924			0.4076[b]		0.579[b]
	0.5939			0.4061[c]		0.617[c]
	0.5992			0.4008[d]		0.620[d]
H_{II}	0.6009			0.3991[a]	O_{II}–H_{II}	0.609[a]
	0.5992			0.4008[b]		0.619[b]
	0.5937			0.4063[c]		0.616[c]
	0.5992			0.4008[d]		0.620[d]
O_I	1.6215	5.3485		−0.9701[a]	Pt–Cl_I	0.717[a]
	1.6285	5.4042		−1.0327[b]		0.914[b]
	1.6215	5.2996		−0.9211[c]		0.534[d]
	1.6200	5.3327		−0.9527[d]		0.718[a]
O_{II}	1.6216	5.3489		−0.9706[a]	Pt–Cl_{II}	0.533[d]
	1.6200	5.3327		−0.9527[b]		
	1.6218	5.2953		−0.9171[c]		
	1.6200	5.3327		−0.9527[d]		
Cl_I	1.8524	4.3978		0.7498[a]		
	1.8456	5.1326		0.0218[b]		
	–	–		–		
	1.8613	5.5367		0.3980[d]		
Cl_{II}	1.8522	4.3981		0.7496[a]		
	–	–		–		
	–	–		–		
	1.8612	5.5367		−0.3982[d]		
Pt	0.4485	0.8486	1.2893	7.4134[a]		
	0.4463	0.6609	1.0146	7.8782[b]		
	0.3405	0.3069	0.6635	8.6890[c]		
	0.6591	0.8921	8.5948	−0.1459[d]		

[a] *cis*-[PtCl$_2$(NH$_3$)$_2$]–silica system.
[b] *cis*-[PtCl(NH$_3$)$_2$]$^+$–silica system.
[c] *cis*-[Pt(NH$_3$)$_2$]$^{2+}$–silica system.
[d] Isolated silica or isolated *cis*platin.

48%, 65% and 92%, respectively. Consequently, for *cis*-[Pt(NH$_3$)$_2$]$^{2+}$ adsorption the major changes are produced in Pt orbital populations.

In general, it is observed an electron transfer to the *cis*platin molecule and the complexes to the surface (see Table 1).

The new interactions are formed at expenses of the OH bonds (see Table 1). When Cl–H interactions are present (during *cis*-[PtCl$_2$(NH$_3$)$_2$] and *cis*-[PtCl(NH$_3$)$_2$]$^+$ adsorption), the OH bond strength is reduced between 1.7 and 7.0% comparing with the OH bond in the isolated surface. When Pt–O interactions are present (during *cis*-[Pt(NH$_3$)$_2$]$^{2+}$ adsorption), the OH bond strength is lightly increased by 1.1% after adsorption. On the other hand, the Pt–Cl bond of *cis*-[PtCl$_2$(NH$_3$)$_2$] and *cis*-[PtCl(NH$_3$)$_2$]$^+$ is strengthen between 35 and 71% after adsorption.

5. Conclusions

The adsorption of *cis*platin on a SiO$_2$(111) hydrated surface was investigated by tight binding calculation. Starting from the optimization of the adsorption geometries for the drug and its complexes, we were able to reproduce the main characteristics of the adsorption process that allow us to show a possible way for the molecule/fragments adsorption. We have also analyzed the nature of the drug–carrier bonding and the changes observed in the electronic structure upon adsorption. Except those molecular orbitals lying much lower in energy, the rest are modified showing the molecule–surface interaction. We have computed the new bondings by the OP and COOP curves. The new interactions are formed at expenses of the OH bonds. One of the major finding are the Cl–H interaction for *cis*-[PtCl$_2$(NH$_3$)$_2$] and *cis*-[PtCl(NH$_3$)$_2$]$^+$ adsorptions, and the Pt–O interaction for *cis*-[Pt(NH$_3$)$_2$]$^{2+}$ adsorption.

References

[1] P.J. O'Dwyer, J.P. Stevenson, Clinical status of cisplatin, carboplatin, and other platinum-based antitumor drugs, in: B. Lippert (Ed.), Cisplatin, Wiley-VCH, Weinheim, 1999, pp. 31–72.
[2] B. Desoize, C. Madoulet, Crit. Rev. Oncol. Hematol. 42 (2000) 317–325.
[3] Y. Ramos Rodríguez, C. Hernández Castro, Rev. Cenic Cienc. Quím. 40 (1) (2009).
[4] A. Andersson, H. Hedenmalm, B. Elfsson, H. Ehrson, J. Pharm. Sci. 83 (1994) 859–862.
[5] S.J. Berners-Price, T.A. Frenkiel, U. Frey, J.D. Ranford, P.J. Sadler, J. Chem. Soc. Chem. Commun. (1992) 789–791.
[6] S.E. Miller, D.A. House, Inorg. Chim. Acta 161 (1989) 131–137.
[7] S.E. Miller, D.A. House, Inorg. Chim. Acta 166 (1989) 189–197.
[8] S.E. Miller, D.A. House, Inorg. Chim. Acta 173 (1990) 53–60.
[9] J.P. Reedijk, Proc. Natl. Acad. Sci. U.S.A. 100 (2003) 3611–3616.
[10] M.A. Jakupec, M. Galanski, B.K. Keppler, Rev. Physiol. Biochem. Pharmacol. 146 (2003) 1–54.
[11] A. Sigel, H. Sigel (Eds.), Metal Ions in Biological Systems, vol. 42, Marcel Dekker, New York, 2004.
[12] D. Wang, S.J. Lippard, Nat. Rev. Drug Discuss. 4 (2005) 307–320.
[13] J.V. Burda, M. Zeizinger, J. Leszczynski, Comput. Chem. 26 (2005) 907–914.
[14] V. Troger, J.L. Fischel, P. Formento, J. Gioanni, G. Milano, Eur. J. Cancer 28 (1992) 82–86.
[15] R.B. Weiss, Drugs 46 (1993) 360–377.
[16] A. Uchida, Y. Shinto, N. Araki, K. Ono, J. Orthop. Res. 10 (2005) 440–445.
[17] K. Ajima, T. Murakami, Y. Mizoguchi, K. Tsuchida, T. Ichihashi, S. Iijima, Yudasaka, ACS Nano 2 (2008) 2057–2064.
[18] M. Vallet-Regi, A. Ramila, R.P. Del Real, J. Perez-Pariente, Chem. Mater. 13 (2001) 308–311.
[19] J. Zhao, F. Gao, Y. Fu, W. Jin, P. Yang, D. Zhao, Chem. Commun. 752 (2002).
[20] T. Yotsuyanagi, M. Usami, Y. Noda, M. Nagata, Int. J. Pharm. 246 (2002) 95–104.
[21] M. Pavelka, M.F.A. Lucas, N. Russo, Chem. Eng. J. 13 (2007) 10108–10116.

[22] V.J. Da Silva, L.A.S. Costa, H.F. Dos Santos, Int. J. Quantum Chem. 108 (2008) 401–414.
[23] T. Zimmermann, J.V. Burda, Interdiscip. Sci. Comput. Life Sci. 2 (2010) 98–114.
[24] Z. Chval, M. Sip, J. Mol. Struct. 532 (2000) 59–68.
[25] Y. Zhang, Z. Guo, X.Z. You, J. Am. Chem. Soc. 123 (2001) 9378–9387.
[26] K.J. Naidoo, G. Klatt, K.R. Koch, D.J. Robinson, Inorg. Chem. 41 (2002) 1845–1849.
[27] L.A.S. Costa, W.R. Rocha, W.B. De Almeida, H.F. Dos Santos, J. Chem. Phys. 118 (2003) 10584–10592.
[28] J.V. Burda, M. Zeizinger, J. Leszczynski, J. Chem. Phys. 120 (2004) 1253–1262.
[29] N.S. Hush, J. Schamberger, G.B. Bacskay, Coord. Chem. Rev. 249 (2005) 299–311.
[30] R. Hoffmann, W.N. Lipscom, J. Chem. Phys. 36 (1962) 2179–2195.
[31] R. Hoffmann, J. Chem. Phys. 39 (1963) 1397–1412.
[32] M.H. Whangbo, R. Hoffmann, J. Am. Chem. Soc. 100 (1978) 6093–6098.
[33] A. Anderson, J. Chem. Phys. 62 (1975) 1187–1188.
[34] G. Landrum, W. Glassey, Yet Another Extended Hückel Molecular Orbital Package (YAeHMOP), Cornell University, Ithaca, NY, 2004.
[35] A. Anderson, R. Hoffmann, J. Chem. Phys. 60 (1974) 4271–4273.
[36] A. Anderson, J. Electroanal. Chem. Interfacial Electrochem. 280 (1990) 37.
[37] J.H. De Boer, J.M. Vleekens, Proc. K. Ned. Akad. We. 61 (1958) 85.
[38] M.M. Branda, R. Montani, N. Castellani, Surf. Sci. 341 (1995) 295.
[39] A. Juan, D. Damiani, C. Pistonesi, Appl. Surf. Sci. 161 (2000) 417–425.
[40] G.H. Milburn, M.R. Truter, J. Chem. Soc. A (1966) 1609.
[41] R. Shandles, E.O. Schlemper, R.K. Murmann, Inorg. Chem. 10 (1971) 2785–2789.
[42] A. Robertazzi, J.A. Platts, J. Comput. Chem. 25 (2004) 1060–1067.
[43] J.K. Park, B.G. Kim, Bull. Korean Chem. Soc. 27 (2006) 1405–1417.
[44] S. Hadi, J. Mat. Dan Dains 11 (4) (2006).
[45] J. Kai-Chi Lau, D.V. Deubel, J. Chem. Theory Comput. 2 (2006) 103–106.